



Cyclo(RGDfK) Functionalized Spider Silk Cell Scaffolds: Significantly Improved Performance in Just One Click

David Harvey, Gemma Bray, Francesco Zamberlan, Mahetab Amer, Sara L. Goodacre, and Neil R. Thomas*

Recombinant spider silk has the potential to provide a new generation of biomaterial scaffolds as a result of its degree of biocompatibility and lack of immunogenicity. These recombinant biomaterials are, however, reported to exhibit poor cellular adhesion which limits their potential for use in applications such as tissue engineering and regenerative medicine. In this study, a simple chemical functionalization approach is described that specifically addresses this issue and significantly improves the adhesion of human mesenchymal stem cells (CiMSCs) to a recombinant spider silk biomaterial. This utilizes copper-catalyzed or strain-promoted azide–alkyne cycloaddition (CuAAC/SPAAC) “click” chemistry to covalently attach cyclo(RGDfK) peptides to the azide group of L-azidohomoalanine, a methionine analogue previously site specifically incorporated into the primary sequence of a thioredoxin (TRX)-tagged silk fusion protein, TRX-4RepCT, to give TRX^{3Aha}-4RepCT^{3Aha}. This method is used to produce cyclo(RGDfK) functionalized films and macroscopic fibers. Over 24 h, cyclo(RGDfK) functionalized TRX^{3Aha}-4RepCT^{3Aha} films and 4RepCT^{3Aha} fibers display significantly improved performance in CiMSC culture, yielding far greater cell numbers than the controls. This approach circumvents the previously observed lack of cell adhesion, thus allowing spider silk derived biomaterials to be used where such adhesion is critical, in tissue engineering, regenerative medicine and wound healing.

Tissue engineering is a rapidly advancing interdisciplinary field of research that utilizes both man-made and natural polymeric materials as scaffolds and supports that improve the culture of mammalian cells. Prominent examples of natural materials include the extracellular matrix (ECM) proteins collagen and elastin. Both have been extensively studied and processed into several different morphologies including gels and fibrous mats that support the culture of mammalian cells.^[1] However, issues such as batch to batch variation, disease transfer, and immunogenicity have been reported that arise from their animal origin.^[2,3] Recombinantly produced spider silk proteins (“spidroins”) are non-animal alternatives that combine material properties such as strength with those of biocompatibility and a lack of immunogenicity and pyrogenicity. Despite this, the ability of recombinant spidroins, specifically those based upon dragline silk, to support mammalian cells has previously been shown to be poor because of the lack of interaction between the cultured cells, and the silk material.^[4] A common

approach to improve cellular adhesion is to decorate the biomaterial with functional ligands, such as peptide based ECM mimics.^[5–9] One such peptide is the ECM derived arginine-glycine-aspartate (RGD) peptide which selectively binds both a and b subunits of integrins found on mammalian cell surfaces.^[10] This sequence has previously been incorporated, at the genetic level, into the primary sequence of dragline silk spidroins in the form of linear RGD motifs, or the peptide has been chemically conjugated in a non-specific way with reactive amino acid sidechains such as lysine, aspartate, glutamate, tyrosine,^[11,12] and cysteine.^[11,12] Incorporation of RGD and of other peptide motifs, using these kinds of strategy, has been shown to improve mammalian cellular adhesion.^[13] These approaches are, however, limited by the availability of reactive sidechains within spidroins, and by the highly repetitive and extraordinarily high guanine-cytosine content of the silk, which makes the introduction of RGD motifs difficult. Introducing extrinsic sequences may also change the overall structure of the spidroin and thus affect properties such as solubility or tendency to aggregate, with consequent changes

Dr. D. Harvey, Dr. F. Zamberlan, Prof. N. R. Thomas
The Biodiscovery Institute
School of Chemistry
University of Nottingham
University Park, Nottingham NG7 2RD, UK
E-mail: Neil.Thomas@nottingham.ac.uk

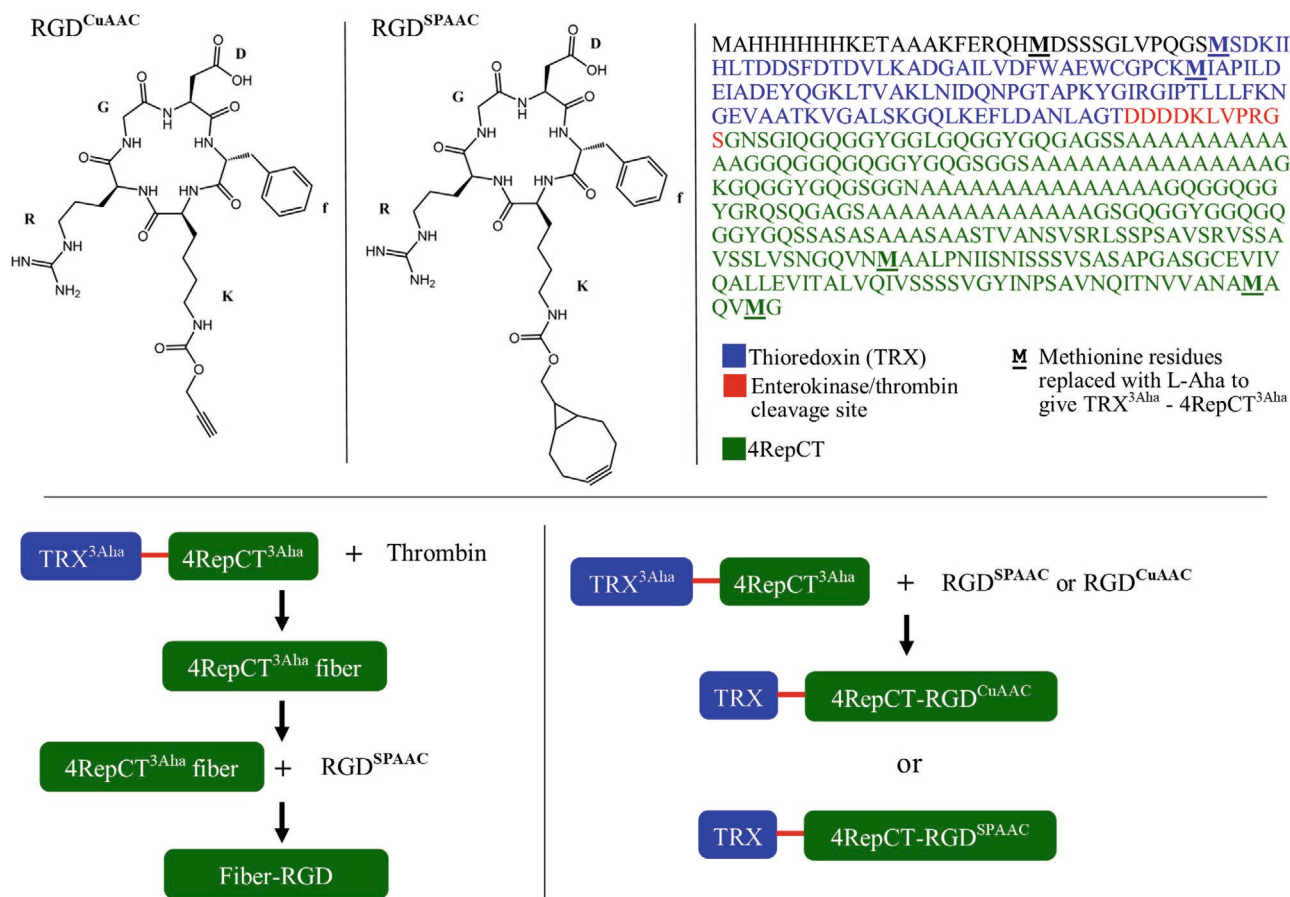
G. Bray and Dr. M. Amer
The Biodiscovery Institute
School of Pharmacy
University of Nottingham
University Park, Nottingham NG7 2RD, UK

Prof. S. L. Goodacre
School of Life Sciences
University of Nottingham
University Park, Nottingham NG7 2RD, UK

The ORCID identification number(s) for the author(s) of this article can be found under <https://doi.org/10.1002/mabi.202000255>.

© 2020 The Authors. Published by Wiley-VCH GmbH. This is an open access article under the terms of the Creative Commons Attribution License, which permits use, distribution and reproduction in any medium, provided the original work is properly cited.

DOI: 10.1002/mabi.202000255



Scheme 1. Functionalization of 4RepCT^{3Aha} fiber and TRX^{3Aha}-4RepCT^{3Aha} soluble fusion protein with cyclo(RGDfK) peptide alkynes. RGD^{CuAAC}; cyclo(RGDfK) peptide conjugated via CuAAC. RGD^{SPAAC}; cyclo(RGDfK) peptide conjugated via SPAAC. Top right panel: sequence of TRX-4RepCT fusion protein, methionine residues swapped for L-Aha are in bold, and underlined (M). Bottom left panel: production of fibers from TRX^{3Aha}-4RepCT^{3Aha} fusion protein and functionalization with RGD^{SPAAC} to give RGD-functionalized fibers (fiber-RGD). Bottom right panel: functionalization of soluble TRX^{3Aha}-4RepCT^{3Aha} fusion protein with RGD^{CuAAC} or RGD^{SPAAC} to produce RGD-functionalized soluble silk fusion protein (TRX-4RepCT-RGD^{CuAAC} or TRX-4RepCT-RGD^{SPAAC})

in physical, and mechanical properties of the spidroin material. Conventional chemical conjugation that targets reactive amino acid sidechains, avoids problems arising from altering the underlying peptide sequence, and can allow the covalent attachment of a wider range of functional ligands, such as organic or inorganic small molecules. The approach is limited, however, by the availability of reactive residues as well as by practical challenges such as reactive ligand instability (hydrolysis of NHS (*N*-hydroxy succinimide) esters for example)^[14] Perhaps more significantly, difficulties also lie with making the modification site specific because it requires sidechains to be accessible, and suitably bioorthogonal to the rest of the protein. Cysteine residues are often targeted owing to their low abundance and defined Michael-addition chemistry with maleimide-tagged ligands.^[15] Unfortunately cysteine-maleimide conjugates have been reported to undergo thiol exchange reactions, de-conjugating the ligand from the protein thus raising concerns over longterm conjugate stability.^[16] Moreover, targeting cysteines may not be appropriate if they form stabilizing disulfide bridges with other cysteines. This is a particular problem for dragline spidroins, including

TRX-4RepCT (sequence shown in **Scheme 1**), that have a C-terminal domain. This domain contains a highly conserved cysteine residue that has been shown, through its substitution by site-directed mutagenesis, to be important in stabilizing C-terminal dimerization, and therefore fiber formation.^[17]

We have previously demonstrated the incorporation of the bioorthogonal methionine analogue, L-azidohomoalanine (L-Aha), into the miniature dragline spidroin TRX-4RepCT (giving TRX^{3Aha}-4RepCT^{3Aha}) using a methionine auxotrophic *E. coli* strain (DL41).^[18] The azide sidechain of L-Aha facilitates the functionalization of TRX^{3Aha}-4RepCT^{3Aha} using “click” chemistry. This method overcomes the challenges associated with conventional chemical functionalization approaches, by providing a bioorthogonal, and site-specific sidechain to target, tolerating a wide scope of reaction conditions, and achieving functionalization in one step. In the present study we use our method to functionalize TRX^{3Aha}-4RepCT^{3Aha} with L-glycine-L-aspartate-D-phenylalanine-L-lysine (cyclo(RGDfK)), a peptide that improves cell adhesion. We demonstrate copper(I)-catalyzed azide-alkyne cycloaddition (CuAAC), as shown in previous work with alkyne modified levofloxacin, and we further

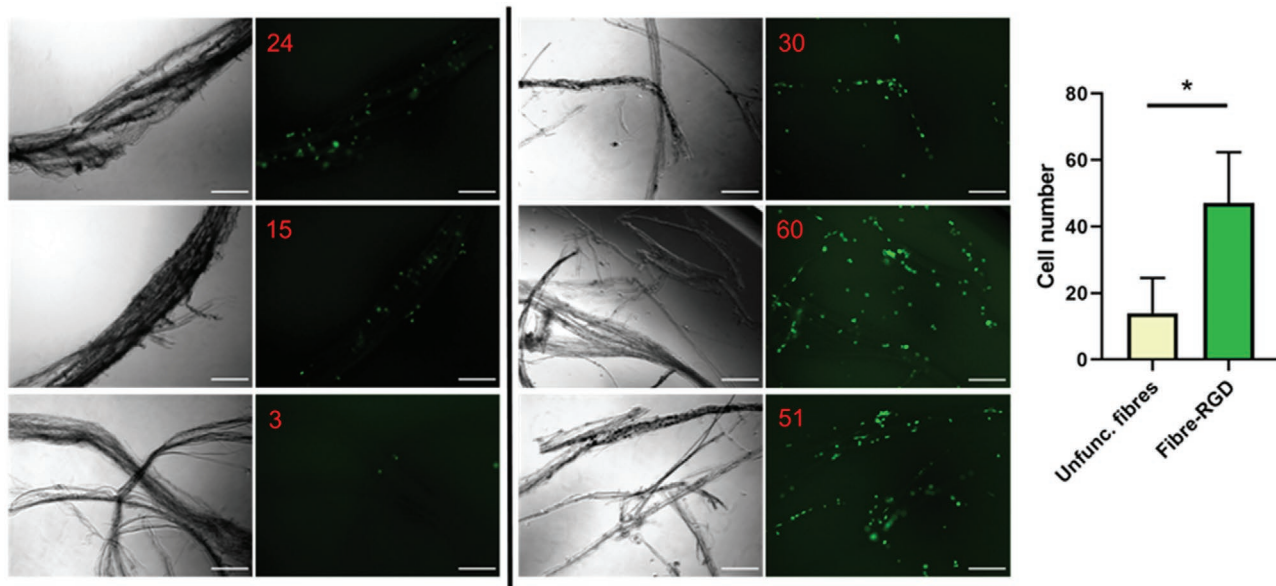


Figure 1. Images taken after 24 h culture of MSC(GFP) cells seeded onto unfunctionalized 4RepCT^{3Aha} fibers and fiber-RGD. Left hand panel: phase contrast and fluorescence images of MSC(GFP) cells cultured on unfunctionalized 4RepCT^{3Aha} fibers. Right hand panel: phase contrast and fluorescence image of MSC(GFP) cells cultured on fiber-RGD. Cell count displayed in red at the top left corner of each fluorescence image. Scale bar (white line) displayed in bottom right corner of each image represents 500 μ m. Bar chart displaying average number of cells counted for each fiber type on far right. Data is mean of $n = 3 \pm$ standard deviation, $p = 0.0375$.

extend our study to use copper-free strain promoted azide-alkyne cycloaddition (SPAAC)-mediated conjugation for the first time with this minispidroin. We demonstrate both copper catalyzed and strain promoted (copper free) addition with soluble spidroin protein that retains its thioredoxin solubility tag (TRX^{3Aha}-4RepCT^{3Aha}) and also with spidroin protein (4RepCT^{3Aha}) that has self-assembled into fibers following cleavage and removal of the thioredoxin (Scheme 1).

As shown in Scheme 1, the soluble fusion protein TRX-4RepCT, contains six methionine residues, three in the TRX, and three in the 4RepCT. All of these are replaced with L-Aha during the expression of TRX^{3Aha}-4RepCT^{3Aha} giving six azide functional groups per fusion protein molecule.^[18] In fiber form, there are three azide groups per protein molecule due to the enzymatic removal of the TRX^{3Aha} solubility tag in order to initiate silk fiber self-assembly.^[18] Cyclo(RGDfK) peptides (RGD-CuAAC and RGD^{SPAAC}) were chosen to functionalize soluble TRX^{3Aha}-4RepCT^{3Aha}, and 4RepCT^{3Aha} fibers because of their reported increased stability, binding affinity, and resistance to proteolysis when compared to linear RGD sequences. This results from the favorable conformational rigidity of the cyclic peptide and incorporation of a non-proteinogenic D-phenylalanine residue.^[19,20] Both cyclo(RGDfK) functionalized films and fibers were subsequently shown to perform better than their unfunctionalized counterparts in the support of growth of human mesenchymal stem cells (CiMSCs and CiMSC(green fluorescent protein) respectively).

Fibers assembled from enzymatically digested TRX^{3Aha}-4RepCT^{3Aha} were functionalized with the RGD^{SPAAC} peptide (to give fiber-RGD) and assessed for their ability to support the adherence and growth of MSC(GFP)s against unfunctionalized 4RepCT^{3Aha} fibers. After a 24-h incubation period,

both functionalized and unfunctionalized fibers were observed using phase contrast, and fluorescence microscopy (Figure 1). Both fiber types were seen clearly under phase contrast and when excited with 400 nm light, the CiMSC(GFP)s were observed to follow the architecture of the silk fibers. Manual cell counts after 24 h incubation revealed that the unfunctionalized 4RepCT^{3Aha} fibers retained significantly fewer CiMSC(GFP) cells than their RGD functionalized counterparts (counts across all replicates were 42 (unmodified 4RepCT^{3Aha}) versus 141 cells (cyclo(RGDfK) modified 4RepCT^{3Aha}) respectively, unpaired t test $p > 0.0375$). Furthermore, the RGD-fiber CiMSC(GFP)s exhibited a more easily observed, flattened needle-like morphology which is indicative of good cellular adhesion.

A volume containing 25 000 CiMSCs (13 157 cells cm^{-2}) was used to seed CuAAC or SPAAC mediated cyclo(RGDfK) functionalized 4RepCT^{3Aha} films (TRX-4RepCT-RGD^{CuAAC} and TRX-4RepCT-RGD^{SPAAC} respectively). Seeded films were observed after 24 h to assess film performance. The functionalized films, TRX-4RepCT-RGD^{CuAAC}, and TRX-4RepCT-RGD^{SPAAC}, were tested individually (Figure 2, left-hand and middle panels) or in parallel (Figure 2, right-hand panel) against unfunctionalized 4RepCT^{3Aha} films, a positive control (tissue culture treated polystyrene (TCTP)), and a negative control (non-tissue culture treated polystyrene, NTCTP). After a 24-h incubation period, the total number of living cells present on each of the films was quantified using the PrestoBlue assay. The number of cells seeded onto the films (25 000) was subtracted from the total number of cells obtained from the assay to give an increase or decrease in cell number for each film type. Cells cultured on NTCTP and unfunctionalized TRX^{3Aha}-4RepCT^{3Aha} films were significantly reduced in number after 24 h incubation.

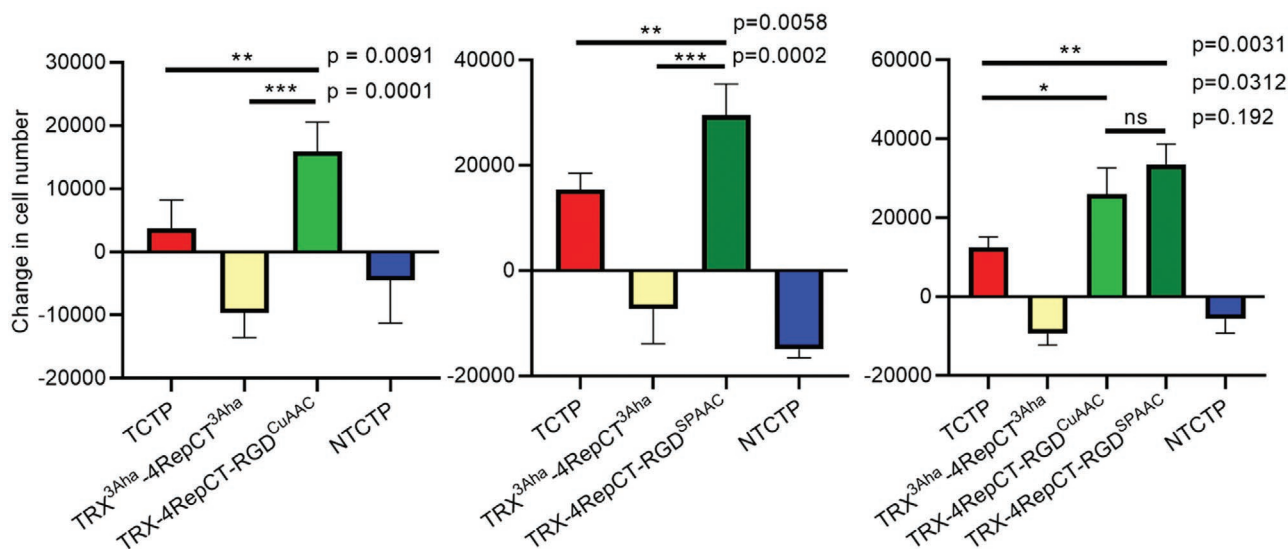


Figure 2. Change in CiMSC number after 24 h incubation with tissue culture treated polystyrene (TCTP), non-tissue culture treated polystyrene, (NTCTP), unfunctionalized silk films (TRX^{3Aha}-4RepCT^{3Aha}), copper catalyzed, RGD functionalized silk film (TRX-4RepCT-RGD^{CuAAC}), and strain promoted, RGD, functionalized silk film (TRX-4RepCT-RGD^{SPAAC}). The standard cell culture material TCTP acts as a positive control for cell growth. NTCTP is not expected to be favourable to cell growth and acts as a negative control. Left-hand bar chart represents a single experiment where only copper catalyzed RGD functionalized silk films were included. The middle bar chart represents an experiment where only strain promoted, RGD functionalized silk films were included. The right-hand bar chart represents an experiment where silk produced using both types of functionalization with RGD peptide were included in the same experiment. Culture conditions for each experiment are displayed along the x-axis of each bar chart. Data is the mean of $n = 4 \pm$ standard deviation.

Conversely, both types of RGD functionalized film resulted in a large, positive change in cell number that was significantly greater than the unfunctionalized films and even the TCTP positive control across each experiment. Interestingly, the TRX-4RepCT-RGD^{SPAAC} films produced greater cell numbers when compared to TRX-4RepCT-RGD^{CuAAC} films across experiments. When tested in parallel, TRX-4RepCT-RGD^{SPAAC} films yielded a higher cell number than TRX-4RepCT-RGD^{CuAAC}; however, this difference was not significant (Figure 2, right-hand panel).

The greatly improved performance of TRX-4RepCT-RGD^{CuAAC} and TRX-4RepCT-RGD^{SPAAC} films was reflected in the confluency and morphology of the CiMSC cultures after 24 h. As shown in Figure 3, the NTCTP, and unfunctionalized TRX^{3Aha}-4RepCT^{3Aha} conditions do not display indications of good cellular adhesion, with rounded cells, clumps of cells, and large areas of empty space. In contrast, TCTP, and wells containing TRX-4RepCT-RGD^{CuAAC} or TRX-4RepCT-RGD^{SPAAC} films displayed CiMSC monolayers of high confluency. Furthermore, the flattened fibroblastic morphologies of the CiMSCs in the RGD functionalized film conditions, and in the TCTP, both indicate good cellular adhesion, signalling the ability of the cells to exploit the cyclo(RGDfK) peptides on the film surface. However, gaps in the monolayer were observed in the TCTP, and to a lesser extent, the TRX-4RepCT-RGD^{CuAAC} conditions indicating that slightly fewer cells adhered to the well/film surface when compared to the TRX-4RepCT-RGD^{SPAAC} condition. These observations are all in agreement with the PrestoBlue assay results shown in Figure 2 that demonstrate cell numbers are higher in the presence of cyclo(RGDfK) functionalized silk than on nonfunctionalised silk, that both types of cyclo(RGDfK) functionalized silk perform better than standard tissue culture

plastic, and that the copper free (i.e. strain promoted) functionalized silk film performs best of all.

Water contact angle (WCA) analysis was employed to test for any changes in hydrophobicity following functionalization with the cyclo(RGDfK) peptide. The WCA for scores for unfunctionalized TRX^{3Aha}-4RepCT^{3Aha} films were not significantly different from the functionalized versions TRX-4RepCT-RGD^{SPAAC} and TRX-4RepCT-RGD^{CuAAC} (101.4° versus 95.8° and 99.2° respectively, Figure 4). The values for all the silk films were much more hydrophobic than the reported WCA scores for tissue culture plastic ($\approx 65^\circ$) and for silkworm fibroin films (74–85°). Silkworm spidroins share many similarities with spider silk^[21,22] so the difference in hydrophobicity could be due to subtle differences between the two in their amino acid composition and/or to differences in the experimental conditions under which these respective films were made.

Scanning electron microscopy (SEM) was used to observe the surface of the cyclo(RGDfK)-functionalized and unfunctionalized films (Figure 5). At relatively low magnification it was apparent that there was a difference between the film types. The unfunctionalized TRX^{3Aha}-4RepCT^{3Aha} films produced the least textured films and displayed small raised areas $\approx 5\text{--}20\ \mu\text{m}$ in size (measuring from extremity to extremity) that appeared to be randomly distributed amongst smoother areas. This observation is consistent with previous studies on 4RepCT films; depicting a bumpy/grainy film surface texture, with bumps ranging into the region of $20\ \mu\text{m}$ in size.^[23] TRX-4RepCT-RGD^{SPAAC} films appeared similar to unfunctionalized films, however the 4RepCT-RGD^{SPAAC} films had more raised areas within the field of view. Interestingly, TRX-4RepCT-RGD^{CuAAC} films had the most textured surface. Furthermore, large aggregate structures

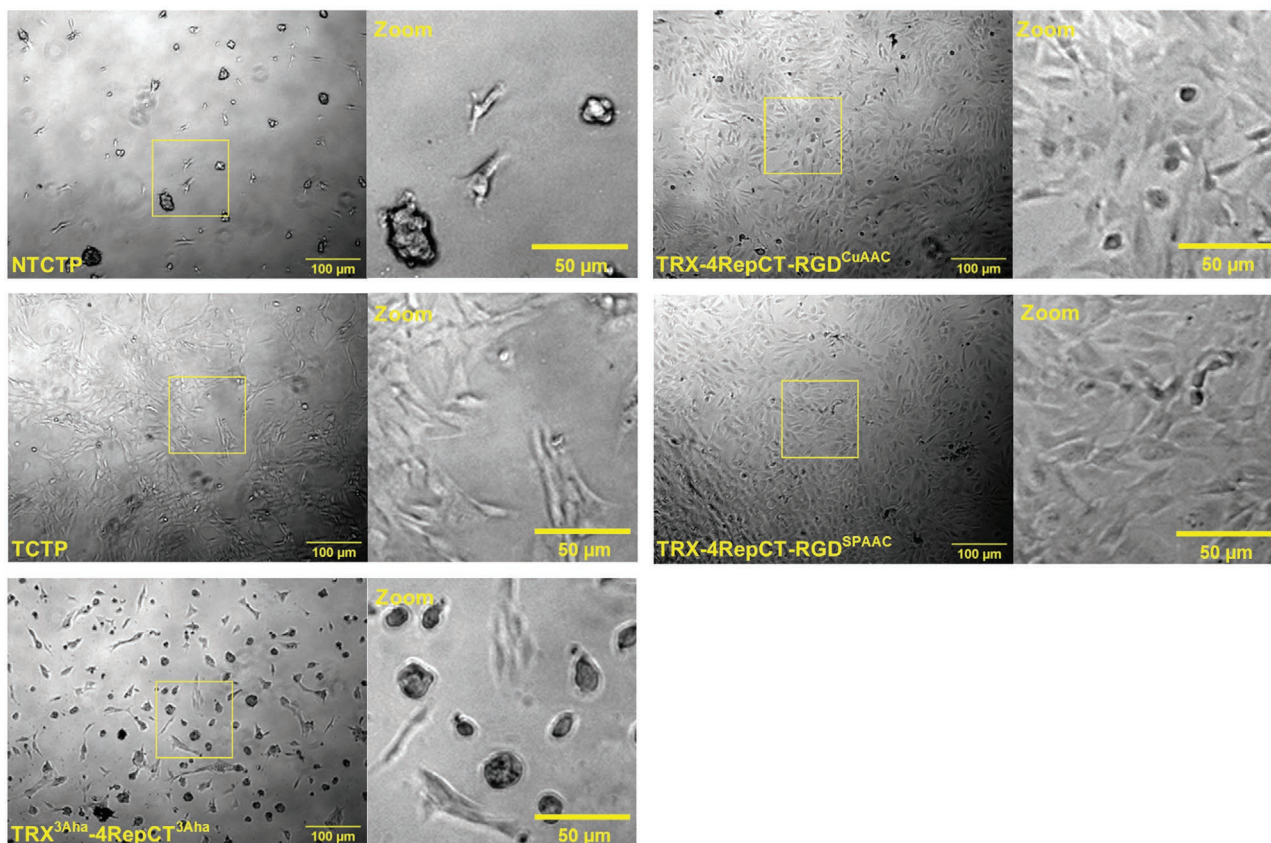


Figure 3. Appearance of CIMSC post 24 h incubation with tissue culture treated polystyrene (TCTP), non-tissue culture treated polystyrene (NTCTP), unfunctionalized silk films, and RGD functionalized silk films. Culture conditions displayed in the bottom left corner of each image; NTCTP (negative control), TCTP (positive control), TRX^{3Aha}-4RepCT^{3Aha} (unfunctionalized silk film), TRX-4RepCT-RGD^{CuAAC} (CuAAC mediated RGD functionalized silk film), and TRX-4RepCT-RGD^{SPAAC} (SPAAC mediated RGD functionalized silk film). Zoomed in image identified by zoom in tope left corner of image. Yellow box indicates location of zoomed in image. Scale bars are given in bottom right of each image.

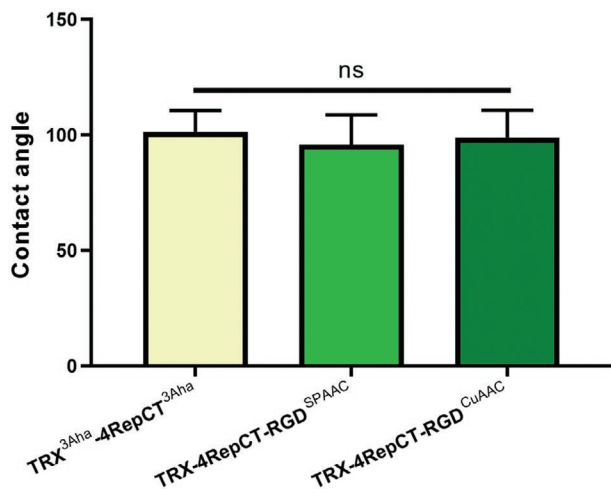


Figure 4. Average WCA for unfunctionalized silk films and RGD functionalized silk films. Film types are shown on the x-axis; unfunctionalized silk films (TRX^{3Aha}-4RepCT^{3Aha}), SPAAC mediated RGD functionalized silk films (TRX-4RepCT-RGD^{SPAAC}), and CuAAC mediated RGD functionalized silk films (TRX-4RepCT-RGD^{CuAAC}). Contact angle displayed on the y-axis. Data is mean of $n = 5 \pm$ standard deviation

of $\approx 30\text{--}50\ \mu\text{m}$ in size (comparable to the diameter of a mammalian cell) were observed, along with a rougher surface in between the bump/aggregate structures.

The need for Cu(I) to catalyze the “click” reaction between TRX^{3Aha}-4RepCT^{3Aha} and the RGD^{CuAAC} peptide leads to the possibility of copper contamination in the final film. Energy Dispersive X-ray Spectrometry (EDS) was used to test both TRX^{3Aha}-4RepCT^{3Aha} and TRX-4RepCT-RGD^{CuAAC} films for the presence of Cu in order to establish whether the toxicity of residual Cu(I) might explain the difference in cell numbers grown in tissue culture. EDS analysis (shown in Figure S1, Supporting Information) did not signal the detection of either Cu(I) or Cu(II) in the films, indicating that the total Cu content was below the detection limit of EDS (0.1% by weight).

In this study, TRX^{3Aha}-4RepCT^{3Aha} fusion protein, and 4RepCT^{3Aha} fibers were functionalized with cyclo(RGDfK) peptides, a known integrin ligand that improves cellular adhesion.^[24] Functionalization was achieved using CuAAC (films only, yielding TRX-4RepCT-RGD^{CuAAC}) and for the first time in recombinant spider silk research, copper-free strain promoted azide-alkyne cycloaddition (SPAAC) (films and fibers, yielding TRX-4RepCT-RGD^{SPAAC}, and fiber-RGD respectively). Both techniques allowed simple and rapid functionalization of the silk material, however SPAAC permitted functionalization

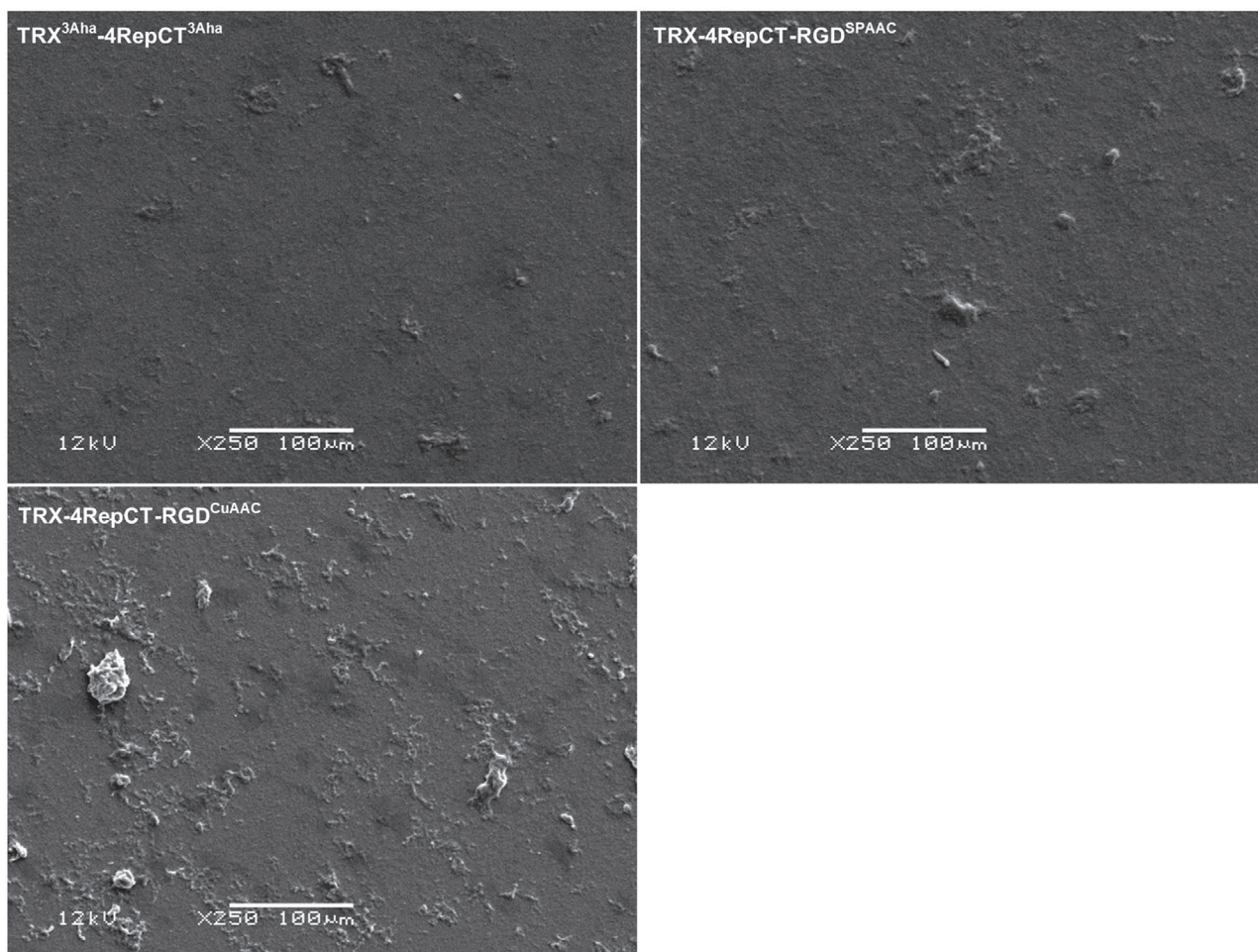


Figure 5. SEM images of an unfunctionalized silk film and RGD functionalized silk films. Film type is given in the top right-hand corner of each image; TRX^{3Aha}-4RepCT^{3Aha} (unfunctionalized silk film), TRX-4RepCT-RGD^{SPAAC} (SPAAC mediated RGD functionalized silk film), TRX-4RepCT-RGD^{CuAAC} (CuAAC mediated RGD functionalized silk film). Images were acquired at 12 kV, 250× magnification. Scale bar represents 100 μm (bottom center of each image)

without a Cu(I) catalyst, therefore avoiding the possibility of copper toxicity through contamination of the final silk material (film or fiber).

Both TRX-4RepCT-RGD^{CuAAC} and TRX-4RepCT-RGD^{SPAAC} formed films within the wells of a 24 well NTCTP plate and were able to tolerate sterilization (in 70% v/v ethanol) and subsequent washing steps without deformation or detaching from the NTCTP surface. Furthermore, fiber-RGD tolerated both autoclave, and ethanol sterilization. This robustness demonstrates their potential to be used reliably as cellular supports or scaffolds.

Functionalization with RGD peptide motifs had a significant impact on performance, with TRX-4RepCT-RGD^{CuAAC}, TRX-4RepCT-RGD^{SPAAC}, and fiber-RGD having greatly improved numbers of cells when compared to unfunctionalized counterparts after 24-h incubation. MSCs express a variety of integrins on their surface so whilst this result was expected based upon data from other studies,^[11,12,25–27] it was not guaranteed because as it was not known whether the cyclo-(RGDfK) peptides would be available for integrin binding after conjugation to fibers or after film formation.^[28] As an example, previous studies that

used *N*-(3-dimethylaminopropyl)-*N'*-ethylcarbodiimide hydrochloride, and NHS to conjugate the GRGDSPC peptide motif (via the N-terminal of the G residue) to acidic residues found in the primary sequence of silk worm fibroin reported no significant difference between functionalized and unfunctionalized films in terms of cell adherence. The authors discussed that their findings may indicate that the RGD-integrin binding mechanism is more complex than previously thought but conceded that the peptide ligand design may have also influenced the result.^[29] Their observations may also be explained by their conjugation strategy. Using the N-terminal amine of G to conjugate the peptide to the film, rather than via a longer linker, may have brought the RGD motif too close to the film surface (glycine is ≈0.42 nm in length), making it much harder for integrins to bind due to unfavorable steric interactions.^[30]

Our study demonstrates that we have overcome the problem described above because we show significant differences between cyclo(RGDfK) functionalized films versus unfunctionalized films and cyclo(RGDfK) functionalized fibers versus unfunctionalized fibers. This indicates that the cyclo(RGDfK) peptides were successfully conjugated and more importantly,

available for integrin binding. In our case, peptide availability was probably aided by the modified flexible lysine side chain linker (shown in Scheme 1), providing enough distance between the peptide, and film/fiber surface. In addition, the short incubation period employed suggested that the cyclo(RGDfK) peptides alone were responsible for the improved performance and this was not a result of CiMSCs producing and depositing ECM proteins on the film or fiber surface. Moreover, the TCTP positive control was significantly outperformed. This demonstrated that the cyclo(RGDfK) functionalized films provided a superior surface to that of standard tissue culture materials for CiMSCs to adhere to and survive on. This result could be explained by the fact that RGD peptide motifs are naturally occurring ligands of integrin receptors, TCTP do not provide these ligands, and so cannot engage integrin receptors as RGD peptides do. The combination of the robust and stable nature of the silk films and the ability to greatly increase cell adhesion/retention with RGD functionalization, showcases the clear potential use of this silk material within cell culture, and tissue engineering.

Functionalized silk fibers (fiber-RGD) also showed potential as a 3D cell culture biomaterial that could be arranged in a mesh to facilitate the growth of layers of cells. However due to their greatly reduced surface area compared to a silk film, the method of cell seeding described in this study is less efficient. To address this problem, cells could be encapsulated into fibers during the fiber formation process as recently described.^[31] However this procedure may not be applicable to all cell types owing to the shear force required to generate fibers, which could influence differentiation.

It is well known that the hydrophobicity of a surface can influence the adhesion of cells.^[32] It was anticipated that the RGD functionalized films would be less hydrophobic than unfunctionalized films (due to charged arginine and aspartate residues).^[26] WCA analysis of all film types revealed that, on average, the cyclo(RGDfK) functionalized films were only subtly less hydrophobic than the unfunctionalized films, with TRX-4RepCT-RGD^{SPAAC} films being the least hydrophobic, but not significantly so. As reported previously, the presence of RGD peptides did change the hydrophobicity of the film surface, but not with statistical significance.^[12] This could be explained by the limited loading capacity of TRX^{3Aha}-4RepCT^{3Aha}, a soluble fusion protein with six azide handles to which the cyclo(RGDfK) peptides can be conjugated; three located within TRX, and three located within the C-terminal of 4RepCT^{3Aha}. Since the amino acid composition of spider silk proteins is dominated by hydrophobic residues, six cyclo(RGDfK) peptides per silk protein molecule is likely insufficient to significantly change bulk properties. Furthermore, it is possible that some of the cyclo(RGDfK) peptide was buried during film formation, and therefore unable to change the wettability of the surface tested.

To supplement the WCA findings the films were observed under SEM and were all shown to have textured surfaces (Figure 3). The overall appearance of the films consisted of smoother areas interspersed with bump-like features in the order of 10 s mm in diameter, however some differences were also observed. Unfunctionalized TRX^{3Aha}-4RepCT^{3Aha} and TRX-4RepCT-RGD^{SPAAC} produced films that had the smoothest features and were comparable to one another in appearance. In contrast, films made from TRX-4RepCT-RGD^{CuAAC} displayed a

rougher surface with large aggregate structures of comparable size to mammalian cells (>20 mm diameter). These larger aggregate structures may have been produced as a result of interactions between TRX^{3Aha}-4RepCT^{3Aha} and “click” reagents necessary to catalyze the CuAAC reaction (2.5 mM sodium ascorbate, 0.5 mM copper sulphate and 2.5 mM Tris(3-hydroxypropyltriazolylmethyl) amine (THPTA)) and carried through to film formation. Therefore, these aggregates may have hindered the binding of CiMSCs to the film surface, contributing to lower cell numbers in comparison to TRX-4RepCT-RGD^{SPAAC} but still providing a significantly superior surface to that of the TCTP.

The use of Cu(I) to catalyze the CuAAC reaction raised concerns of copper ion contamination in TRX-4RepCT-RGD^{CuAAC} films which could exert a toxic effect on the CiMSCs, effecting cell viability, and total cell number. Subsequent EDS analysis of TRX-4RepCT-RGD^{CuAAC} versus unfunctionalized films was performed to detect copper contamination. However, it was revealed that copper content, in both film types, was below detectable levels (0.1% by weight). This indicated that copper was removed by dialysis (post cyclo(RGDfK) conjugation), washing steps involved in film formation, and perhaps aided by using THPTA (as an efficient Cu(I) chelating agent) during the CuAAC reaction. Consequently, copper toxicity does not seem responsible for the lower cell numbers observed for TRX-4RepCT-RGD^{CuAAC} films, instead this appears more likely to have been caused by increased roughness of the TRX-4RepCT-RGD^{CuAAC} film surface.

In conclusion, we have shown copper catalyzed, and strain promoted “click” chemistry mediated functionalization of 4RepCT^{3Aha}, in soluble and fiber form, with cyclo(RGDfK) peptides. This highly flexible approach yielded functionalized materials that performed significantly better than their unfunctionalized counterparts in CiMSC culture. After 24 h, functionalized materials retained greater cell numbers, and can therefore reduce the time taken to reach confluency; a valuable capability when culturing precious primary cells often used in tissue engineering, and regenerative medicine. In addition, we have previously shown that by blending functionalized soluble silk protein, it is possible to create multi-labeled silk materials.^[18] Similarly, multi-labeled TRX^{3Aha}-4RepCT^{3Aha} films or 4RepCT^{3Aha} fibers, functionalized with a suite of peptides or molecules, could be made simply by blending controlled ratios of soluble functionalized silk protein together. This could be used to produce 2D and 3D silk materials of increasing complexity that more closely mimic tissue specific niches.

Experimental Section

Chemical Synthesis Methods: Cyclo(RGDfK) peptides (Peptides International, Kentucky, USA) were chemically modified to bear either a propargyl or bicyclononyne (BCN) functional group, giving RGD^{CuAAC} or RGD^{SPAAC} respectively. Expanded chemical synthesis methods relating to the preparation of the functional groups can be found in the supporting information along with information on all the analytical methods used.

Synthesis of RGD^{CuAAC}: Propargyl *p*-nitrobenzyl carbonate (2.1 mg, 4.97 mmol, 1.26 equivalent.) was dissolved in 1 mL dimethylformamide (DMF) and the resulting solution was used to dissolve cyclo(RGDfK) (5 mg, 8.3 mmol). Triethanolamine (TEA) was added dropwise until

the solution turned clear yellow. It was left stirring for 18 h at room temperature. The reaction was followed by high resolution mass spectrometry (HRMS) to determine reaction completion. The desired product was purified using high performance liquid chromatography (HPLC), equipped with a semipreparative Agilent Eclipse XDB-C18 column, and displayed a retention time of 13.40 min (full method shown in the supporting information). The identity of the fraction collected at 13.40 min was confirmed by HRMS (ESI): $C_{31}H_{43}N_9O_9$ calculated [M + H]: 686.3257; found [M + H]: 686.3265. Collected fractions were freeze-dried yielding 0.9 mg (26%) of the target compound.

Synthesis of RGD^{SPAAC}: BCN carbonate (4.64 mg, 14.73 μ mol, 1.77 equivalent) was dissolved in 1 mL DMF and the resulting solution was used to dissolve cyclo(RGDfK) (5 mg, 8.3 mmol). TEA was added dropwise until the solution turned clear yellow. It was left stirring for 18 h at room temperature. The reaction was followed by HRMS to determine reaction completion. The desired product was purified using HPLC, equipped with a semipreparative Agilent Eclipse XDB-C18 column, and displayed a retention time of 16.50 min. The identity of the fraction collected at 16.50 min was confirmed by HRMS (ESI): $C_{38}H_{53}N_9O_9$ calculated [M+H]: 780.4039; found [M+H]: 780.4061. Collected fractions were freeze-dried yielding 3.9 mg (60%) of the target compound.

Expression and Purification of TRX^{3Aha}-4RepCT^{3Aha}: TRX^{3Aha}-4RepCT^{3Aha} was expressed and purified as previously described.^[1] After purification the protein was transferred to dialysis tubing (SpectraPor, Spectrum Labs, USA) with a molecular cut-off of 30 000 Da and dialyzed overnight against 20 mM Tris buffer pH 8.0. Following dialysis, TRX^{3Aha}-4RepCT^{3Aha} was concentrated using a spin concentrator with molecular weight cut-off of 10 000 Da (Amicon) until a concentration of 1–3.5 mg mL⁻¹ (25–87.6 mM) was reached.

Assembly of 4RepCT^{3Aha} Fibers: Fibers were made through the enzymatic removal of thioredoxin from 4RepCT^{3Aha}. Solutions containing 1.5 mg mL⁻¹ of TRX^{3Aha}-4RepCT^{3Aha} were made in sealed fraction collection tubes and incubated with thrombin (1:1000 w/w, 1 mg thrombin/1 mg TRX^{3Aha}-4RepCT^{3Aha}) for 2–3 h at 37 °C. Tubes were gently agitated back and forth in the incubator.

Conjugation of RGD^{SPAAC} to 4RepCT^{3Aha} Fibers: Conjugation of RGD^{SPAAC} to 4RepCT^{3Aha} fibers (to give fiber-RGD) was carried out in a reaction containing 180 mL of 20 mM Tris pH 7.5 and 20 mL of 5 mM RGD peptide. Reactions were incubated at room temperature for 2 h with gentle shaking. After incubation, fibers were removed from the reaction tube, and washed with 20 mM Tris pH 7.5 buffer. Fibers were sterilized by autoclave (120 °C, 15 min) and again with 70% (v/v) ethanol.

Conjugation of RGD^{CuAAC} to TRX^{3Aha}-4RepCT^{3Aha}: Conjugation of RGD^{CuAAC} peptide to TRX^{3Aha}-4RepCT^{3Aha} (to give TRX-4RepCT-RGD^{CuAAC}) was carried out in several 100 mL reactions comprised of 60 mL of 32 mM 4RepCT^{3Aha}, 24 mL of 20 mM Tris buffer pH 7.5, 5 mL of 50 mM THPTA, 5 mL of 50 mM sodium ascorbate, 1 mL of 50 mM CuSO₄, and 5 mL of 5 mM RGD^{CuAAC} peptide. The reaction was incubated for 2 h at room temperature with gentle agitation. After incubation the reactions were pooled and dialyzed overnight against 20 mM Tris buffer pH 8.0 to remove excess reactants.

Conjugation of RGD^{SPAAC} Peptide to TRX^{3Aha}-4RepCT^{3Aha}: Conjugation of RGD^{SPAAC} peptide to TRX^{3Aha}-4RepCT^{3Aha} (to give TRX-4RepCT-RGD^{SPAAC}) was carried out in several 100 mL reactions comprised of 50 mL of 87 mM 4RepCT^{3Aha}, 40 mL of 20 mM Tris buffer pH 7.5, and 10 mL 5mM RGD^{SPAAC} peptide. The reaction was incubated at room temperature for 2 h with gentle agitation. After the reactions were pooled and dialyzed against 20 mM Tris buffer pH 8.0 to remove excess reactants.

Film Formation: Following overnight dialysis 200 μ g of soluble TRX^{3Aha}-4RepCT^{3Aha}, TRX-4RepCT-RGD^{CuAAC}, and TRX-4RepCT-RGD^{SPAAC} was used to construct films on microscope slides (for WCA and energy dispersive X-ray spectroscopy (EDX) analysis) or within a 24 well non-tissue culture plastic (NTCTP) well plate (Falcon) (for cell culture). All films were made by evaporating the buffer solution using either a desiccator chamber filled with CaCl₂ (films on microscope slides) or sterile air within a cell culture hood (films in well plates). After film formation films were soaked in 1 mL 70% (v/v) ethanol for 10 min to

sterilize the film and removed by aspiration. All films were subsequently washed three times with 1 mL sterile phosphate buffered saline to remove traces of tris buffer and ethanol. Finally, for films in well plates, 1 mL of Dulbecco's modified eagle medium (DMEM) (Gibco) was added into the wells, and the plate transferred to an incubator set at 37 °C 5% CO₂ to allow the media to warm up.

Cell Culture of Commercially Immortalized Mesenchymal Stem Cells (CiMSCs): A vial of commercially immortalized mesenchymal stem cells (CiMSCs) (Japanese Collection of Research Bioresources) were rapidly thawed and subsequently cultured in T75 flasks (Corning Costar). Cells were maintained in DMEM containing 10% (v/v) fetal bovine serum (Sigma Aldrich) and penicillin-streptomycin (100 units) (Sigma Aldrich) and incubated at 37 °C 5% CO₂. Once confluent, cells were passaged using trypsin/EDTA (0.25%/0.02% v/v) (Sigma Aldrich), and their culture continued no further than 8–10 passages.

Culture of CiMSCs on TRX^{3Aha}-4RepCT^{3Aha}, TRX-4RepCT-RGD^{CuAAC} and TRX-4RepCT-RGD^{SPAAC} Films: CiMSCs were harvested from a single T75 flask and counted using a Neubauer improved hemocytometer. A volume of media containing 25 000 CiMSCs was added to wells containing 1 mL pre-warmed media and either the positive control (tissue culture plastic—TCTP control), unmodified TRX^{3Aha}-4RepCT^{3Aha} films, TRX-4RepCT-RGD^{CuAAC} films, TRX-4RepCT-RGD^{SPAAC} films, and the negative control (NTCTP—neg control). After seeding the well plates were returned to the 37 °C 5% CO₂ incubator for 24 h

Culture of CiMSCs on Fiber-RGD: CiMSCs were harvested from a single T75 flask and counted using a Neubauer improved hemocytometer. A volume of media containing 25 000 CiMSCs was added to wells containing 1 mL pre-warmed media and either unfunctionalized 4RepCT^{3Aha} fibers or fiber-RGD. Cells were seeded directly over the fibers to maximize chances of the cells landing on fibers.

Visualization of CiMSCs Growing on Films: After the 24-h incubation period the well plates were removed from the incubator and inspected using a phase contrast microscope (Leica DMRBE). Images were taken at 10 \times magnification using Velocity software (Improvision UK). Scale bars were added using ImageJ (Fiji)

Visualization of Fluorescent CiMSCs Growing on Unfunctionalized and RGD Functionalized 4RepCT^{3Aha} Fibers: After the 24-h incubation period, the fibers were inspected using phase contrast, and fluorescence microscopy at 4 \times magnification (Leica DMRBE). Images of fibers were taken using phase contrast and then under fluorescence conditions (using 400 nm light to excite the expressed GFP) to identify the location of the adhered CiMSCs. Scale bars were added using ImageJ (Fiji)

Fluorescent Cell Counting: The following criteria were applied across fiber samples to ensure fair counting of fluorescent CiMSCs. Fibers were located on the bottom of each well and brought into the sharpest focus possible. This focal plane was applied across all samples. Only sharp defined green dots were counted. Blurred or out of focus fluorescent bodies were not counted since they were out of the fixed focal plane. Blobs or aggregates of cells were counted as one because it was not possible to resolve how many cells were in the aggregates

PrestoBlue Assay: The PrestoBlue assay was used to quantify cell numbers growing on silk films. Old DMEM media was aspirated from each well, replaced with fresh DMEM containing 1 \times PrestoBlue solution (DMEM PrestoBlue), and the well plates returned to the incubator for 2 h. A volume of 200 mL of DMEM PrestoBlue was aspirated from each well and transferred to a black 96 well plate. The fluorescence of the aspirates was determined using a TECAN infinite 200 plate reader and TECAN i-control 1.10.4.0 software using an excitation wavelength of 535 nm and emission wavelength of 615 nm.

Water Contact Angle: WCA measurements were performed on a CAM 200 optical contact angle meter (KSV Instruments Ltd., Finland) using the sessile drop method and CAM 200 image analysis software. Water droplets were placed on each surface and ten images were taken at 1 s intervals. All measurements were made at room temperature. WCAs were calculated using a Young-Laplace fitting function and the resulting right and left contact angles were averaged out. Five repeat measurements were made for each material in triplicate. Measurements are presented as average \pm standard deviation.

Scanning Electron Microscopy: SEM was carried out on a Jeol 6060LV variable pressure scanning electron microscope (Jeol UK Ltd, UK). Before insertion into the chamber, samples were coated in gold using a Leica EM SCD005 Sputter Coater for 300 s. Images were acquired using a voltage of 12 kV at 25×, 100×, 250×, 500×, or 1000× magnification

Energy Dispersive X-Ray Spectroscopy: EDX was conducted on a FEI QUANTA 650 scanning electron microscope in conjunction with an Oxford Instruments X-max 150 detector. Before analysis, sample films on microscope slides were coated with a fine layer of carbon using an Agar Turbo carbon coater. Images of the film edge, center, and part way between edge and center were acquired using a voltage of 20 kV. Within each image three areas were chosen for analysis by EDX, therefore totaling nine EDX analyses per film (see Figure S1, Supporting Information).

Supporting Information

Supporting Information is available from the Wiley Online Library or from the author.

Acknowledgements

This project was funded by a Biotechnology and Biological Sciences Research Council doctoral training studentship (grant number BB/J014508/1) to D.H. and a BBSRC follow-on grant (grant number BB/N012658/1). The authors would like to acknowledge and thank the Nanoscale and Microscale Research Centre (nmRC) and Dr. Elizabeth Steer for help with SEM and EDX analysis. The authors would also like to acknowledge Prof. F. Rose (School of Pharmacy) for access to mammalian cell culture facilities.

Conflict of Interest

The authors declare no conflict of interest.

Keywords

Aha, bioorthogonal, click chemistry, CuAAC, RGD, silk, strain-promoted azide-alkyne cycloaddition

Received: July 22, 2020
Published online: August 31, 2020

- [1] D. Miranda-Nieves, E. L. Chaikof, *ACS Biomater. Sci. Eng.* **2017**, *3*, 694.
[2] R. J. Mullins, C. Richards, T. Walker, *Aust. J. Ophthalmol.* **1996**, *24*, 257.
[3] M. J. Rapaport, *Arch. Dermatol.* **1984**, *120*, 837.

- [4] A. Leal-Egaña, T. Scheibel, *Biotechnol. Appl. Biochem.* **2010**, *55*, 155.
[5] K. Tashiro, G. C. Sephels, B. Weeks, M. Sasakig, G. R. Martin, H. K. Kleinman, Y. Yamada, *J. Biol. Chem.* **1989**, *264*, 16174.
[6] U. Hersel, C. Dahmen, H. Kessler, *Biomaterials* **2003**, *24*, 4385.
[7] Y. Arima, H. Iwata, *Biomaterials* **2007**, *28*, 3074.
[8] A. V. Taubenberger, M. A. Woodruff, H. Bai, D. J. Muller, D. W. Huttmacher, *Biomaterials* **2010**, *31*, 2827.
[9] D. N. Adams, E. Y.-C. Kao, C. L. Hypolite, M. D. Distefano, W.-S. Hu, P. C. Letourneau, *J. Neurobiol.* **2005**, *62*, 134.
[10] R. Pankov, K. M. Yamada, *J. Cell Sci.* **2002**, *115*, 3861.
[11] M. Widhe, U. Johansson, C.-O. Hillerdahl, M. Hedhammar, *Biomaterials* **2013**, *34*, 8223.
[12] S. Wohlrab, S. Müller, A. Schmidt, S. Neubauer, H. Kessler, A. Leal-Egaña, T. Scheibel, *Biomaterials* **2012**, *33*, 6650.
[13] S. Salehi, K. Koeck, T. Scheibel, *Molecules* **2020**, *25*, 737.
[14] G. T. Hermanson, *Bioconjugate Techniques*, Academic Press, San Diego, CA **2008**.
[15] A. Moura, M. A. Savageau, R. Alves, *PLoS One* **2013**, *8*, e77319.
[16] G. Badescu, P. Bryant, J. Swierkosz, F. Khayrzad, E. Pawlisz, M. Farys, Y. Cong, M. Muroi, N. Rumpf, S. Brocchini, A. Godwin, *Bioconjugate. Chem.* **2014**, *25*, 460.
[17] S. Ittah, A. Michaeli, A. Goldblum, U. Gat, *Biomacromolecules* **2007**, *8*, 2768.
[18] D. Harvey, P. Bardelang, S. L. Goodacre, A. Cockayne, N. R. Thomas, *Adv. Mater.* **2017**, *29*, 1604245.
[19] S. J. Bogdanowich-Knipp, S. Chakrabarti, T. J. Siahaan, T. D. Williams, R. K. Dillman, *J. Peptide Res.* **1999**, *53*, 530.
[20] T. G. Kapp, F. Rechenmacher, S. Neubauer, O. V. Maltsev, E. A. Cavalcanti-Adam, R. Zarka, U. Reuning, J. Notni, H. J. Wester, C. Mas-Moruno, J. Spatz, B. Geiger, H. Kessler, *Sci. Rep.* **2017**, *7*, 39805.
[21] S. Rajaraman, G. Subbiahdoss, G. Dhakshinamoorthy, S. Rajakannu, *Asian J. Pharm. Clin. Res.* **2015**, *8*, 229.
[22] X. J. Lian, S. Wang, H. S. Zhu, *Front. Mater. Sci. China* **2010**, *4*, 57.
[23] M. Widhe, H. Bysell, S. Nystedt, I. Schenning, M. Malmsten, J. Johansson, A. Rising, M. Hedhammar, *Biomaterials* **2010**, *31*, 9575.
[24] C. S. Chen, J. L. Alonso, E. Ostuni, G. M. Whitesides, D. E. Ingber, *Biochem. Biophys. Res. Commun.* **2003**, *307*, 355.
[25] D. S. Hwang, S. B. Sim, H. J. Cha, *Biomaterials* **2007**, *28*, 4039.
[26] P. W. Kämmerer, M. Helle, J. Brieger, M. O. Klein, B. Al-Nawas, M. Gabriel, *Eur. Cells Mater.* **2011**, *21*, 364.
[27] E. Bini, C. W. P. Foo, J. Huang, V. Karageorgiou, B. Kitchel, D. L. Kaplan, *Biomacromolecules* **2006**, *7*, 3139.
[28] D. Docheva, C. Popov, W. Mutschler, M. Schieker, *J. Cell. Mol. Med.* **2007**, *11*, 21.
[29] L. Bray, S. Suzuki, D. Harkin, T. Chirila, *J. Funct. Biomater.* **2013**, *4*, 74.
[30] M. Steinhart, *Angew. Chem., Int. Ed.* **2004**, *43*, 2196.
[31] U. Johansson, M. Widhe, N. D. Shalaly, I. L. Arregui, L. Nilebäck, C. P. Tasiopoulos, C. Åstrand, P. O. Berggren, C. Gasser, M. Hedhammar, *Sci. Rep.* **2019**, *9*, 6291.
[32] D. P. Dowling, I. S. Miller, M. Ardhauoui, W. M. Gallagher, *J. Biomater. Appl.* **2011**, *26*, 327.